Journal of Engineering Mathelatics, Vol. 6, No. 3, July 1972
Wolters-Noordhoff Publishing–Groningen
Printed in the Netherlands

The Radial Spreading as a Free Surface Layer of a Vertical Buoyant Jet

H. O. ANWAR

Hydraulics Research Station, Wallingford, Berkshire, England

(Received August 17, 1971)

SUMMARY

When the rising plume in a stagnant ambient fluid impinges the free surface it spreads radially as a surface layer flowing over a pool of heavier liquid. Initially the surface layer in the "entrainment zone" entrains the underlying fluid, but the entrainment decreases with the increasing distance from the "boil". The radius of the entrainment zone depends on the initial buoyancy flux from the nozzle and also on submergence height. It was assumed that the flow in this zone has a self-preserving form. The theoretical results based upon this assumption showed that the maximum velocity and density difference of the layer decreases as powers of radius distance measured from centre of the boil and the depth varies linearly with the radius, so that the sectional Richardon's number based on maximum physical quantities of the section remain unchanged. It was further shown that the coefficient of the entrainment remains constant and is a function of the Richardson's number and the slope of the interface. The theoretical results were compared with those obtained experimentally and fair agreement was obtained.

At the end of the entrainment zone the surface layer enters the "zone of homogeneous flow" in which the layer travels over the underlying fluid and behaves much like a free homogeneous flow over a rigid boundary: the friction at the interface replacing the friction of the boundary. In this zone the mean velocity of the layer in the radial direction was measured and found that it decreases inversely with the increase of radius. The thickness of the layer in the zone of homogeneous flow remains constant and depends, as far as experiments show, greatly on the submergence height.

1. Introduction

When a buoyant effluent is discharged from a submerged pipe into a static (or gently moving) body of water it rises to the surface and dilutes en route. The behaviour of the buoyant jet at some distance from the nozzle is like a convectional plume above a point source, provided the diameter of the nozzle relative to the vertical reach of the buoyant jet is small. The rising column of effluent breaks the free surface at the "boil" and spreads radially over the ambient fluid as a surface layer. This layer entrains more of the ambient fluid as it spreads, and hence it becomes more diluted. Both the dilution and the thickness are of interest to engineers concerned with the disposal of sewage or other wastes into the sea, including the discharge of warmed water from the cooling systems of power stations.

The spread of the surface layer and its dilution depend upon whether the surrounding fluid is moving or at rest. In the latter case the surface layer will mix less with the ambient fluid than in the former case and hence the most severe condition to take into account in the design of a submarine outfall into tidal waters is slack water. This condition of an ambient fluid at rest is considered in the present paper and in this case the entrainment of the underlying fluid by the surface layer decreases with the distance from the "boil" point, where the rising column impinges on the free surface. The surface layer then reaches a final stage within which its density and its thickness remain unchanged. The ultimate thickness of the surface layer, and the radius at which this final stage is reached, depend upon the depth of submergence and the geometry of the outlet, i.e. upon whether it is discharging horizontally or vertically upwards. Rawn and Palmer [1] measured the final thickness of the surface layer and found it to be about $\frac{1}{12}$ of the length of the trajectory of the buoyant jet, when the outlet discharges horizontally. Hart [2], on the other hand, found that the thickness of the layer is about $\frac{1}{6}$ of the submergence when the buoyant jet discharges vertically upwards. Hart also measured the dilution of the surface layer at a distance of about 1 ft from the boil, which was probably within the entrainment zone in some of his model tests. Sharp [3] measured the velocity of the tip of the layer for various horizontal discharges.

In the present investigation, both the "entrainment zone" of the surface layer and its final stage, the "zone of homogeneous flow", were studied. It has been assumed theoretically that the flow in the entrainment zone has a self-preserving form. This means that the flow is geometrically similar at all sections. This was confirmed when the experimental results were compared with the theory. Theoretically it was found that the sectional Richardson's number (defined later) remains unchanged. Further it was found that the coefficient of entrainment (defined as the rate of inflow of the underlying fluid into the surface layer) depends on the sectional Richardson's number and also the slope of the interface, hence it remains constant, because of constant slope of the interface.

In the experimental part of this investigation fresh water was discharged vertically upwards at two different submergence depths into a salt solution at rest. The density of the surface layer was measured at various radial distances from the boil, and also at various depths. From this information the thickness of the layer and its dilution were determined. Measurements were also made of the velocity and the surface slope of the surface layer.

2. Theory

2.1. *Entrainment zone*

The entrainment of the underlying fluid into the moving surface layer will continue to a distance r_e from the "boil" (see Fig. 1 for nomenclature and illustration). Beyond the radius r_e it is assumed that the turbulence has decayed to such an extent that the flow does not entrain the underlying fluid. In this case the surface flow is similar to the type of flow that will occur with a homogeneous fluid. This part of the surface layer will be dealt with later. Firstly various features of the surface flow in the entrainment zone between the "boil" and r_e (see Fig. 1) will be examined.

It will be assumed that the motion in this zone is steady. This means that the tip of the surface layer is sufficiently far from the boil and the underlying fluid is not contaminated by the process of the entrainment. It will be further assumed that the local variation in density remains small relative to some reference density. Thus, the Boussinesque approximation may be made, namely that the density difference between the ambient fluid and surface layer can be neglected except where multiplied by g, the acceleration due to gravity [4]. The equations of motion for a turbulent, incompressible flow of the surface layer with negligible energy dissipation may be written as follows by using the system of co-ordinates shown in Fig. 1.

$$\rho\left(u\frac{\partial u}{\partial r}+v\frac{\partial u}{\partial z}\right)=f-\frac{\partial p}{\partial r}+\frac{1}{r}\frac{\partial}{\partial r}(r\tau)\,. \tag{2.1}$$

The equation of conservation of mass density can be written as follows

$$u\frac{\partial(r\Delta\rho)}{\partial r}+v\frac{\partial(r\Delta\rho)}{\partial z}=-\frac{\partial}{\partial z}(r\overline{v'\Delta\rho'}) \tag{2.2}$$

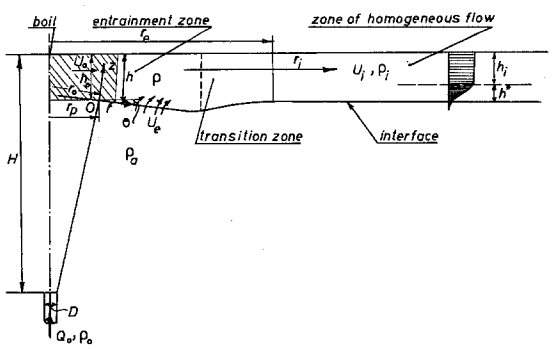

Figure 1. Definition of terms for surface layer.

and the continuity equation can be written in the following form

$$\frac{\partial(ur)}{\partial r} + \frac{\partial(vr)}{\partial z} = 0 . \tag{2.3}$$

In the above equations r and z are natural cylindrical co-ordinates with respective local velocity u and v. f is the body force in the r-direction and τ the Reynolds shear stress. $\Delta\rho = \rho_a - \rho$ with ρ_a and ρ the mass density of the underlying fluid and surface layer respectively and, finally, $\overline{v'\Delta\rho'}$ is the correlation between fluctuation of vertical velocity v and the density differences $\Delta\rho$.

In equation (2.1) the body force f is the component of buoyancy force in the r-direction and can be written

$$f = -g(\rho_a - \rho)\sin\theta \tag{2.4}$$

where θ is the angle of inclination of the interface, $g(\rho_a - \rho)$ is the local buoyancy (local weight density). The second term on the right-hand side of equation (2.1) is the variation of the hydrostatic pressure in the r-direction and can be written

$$\frac{\partial p}{\partial r} = -\frac{\partial}{\partial r}[g(\rho_a - \rho)z] \tag{2.5}$$

The above equation represents the variation of the pressure force on the surface layer due to the change of its density and thickness. In other words, the difference between the hydrostatic pressure on the faces r and $r+dr$. By substituting equations (2.4) and (2.5) into equation (2.1) we obtain

$$ur\frac{\partial u}{\partial r} + vr\frac{\partial u}{\partial z} = -g\frac{\Delta\rho}{\rho_a} r\sin\theta + r\frac{\partial}{\partial r}\left(g\frac{\Delta\rho}{\rho_a} z\right) + \frac{1}{\rho_a}\frac{\partial}{\partial r}(r\tau) . \tag{2.6}$$

In order to proceed with the theoretical development, in the following section we must examine the condition of self-preserving flow in the entrainment zone.

3. Self-preservation

The motion in the vertical plume exhibits a self-preserving flow. This indicates that the conditions of each section above the nozzle are similar. Now, when the flow turns from the vertical direction into a horizontal radial flow it is appropriate to look for the existence of a self-preserving flow, and a reasonable assumption at this stage would be that the velocity distribution depends only on a characteristic velocity and length for that section, and the density distribution depends only on a characteristic density and the same characteristic length for that section, i.e.

$$U = U_s F(\eta), \quad \Delta\rho = \Delta\rho_s G(\eta) \qquad \frac{\tau}{\rho_a} = U_s^2 f_1(\eta), \quad \eta = \frac{z}{h} \tag{3.1}$$

in which U_s and $\Delta\rho_s$ are functions of r alone and h is the depth of layer.

If expressions (3.1) are substituted into equation (2.6), with suitable rearrangement and by making use of equation (2.3), the following form is obtained

$$\frac{h}{U_s}\frac{dU_s}{dr}F^2(\eta) - \frac{dh}{dr}F(\eta)F'(\eta)\eta - \frac{h}{U_s r}\frac{d(U_s r)}{dr}F'(\eta)\int_0^\eta F(\eta)d\eta +$$

$$\frac{dh}{dr}F'(\eta)\int_0^\eta F'(\eta)\eta\,d\eta + \frac{g\dfrac{\Delta\rho_s}{\rho_a}h}{U_s^2}\sin\theta G(\eta) - \frac{d\left(g\dfrac{\Delta\rho_s}{\rho_a}\right)}{dr}\frac{h^2}{U_s^2}G(\eta)\eta -$$

$$\frac{g\dfrac{\Delta\rho_s}{\rho_a}h}{U_s^2}\frac{h}{r}G(\eta)\eta + \frac{dh}{dr}\frac{g\dfrac{\Delta\rho_s}{\rho_a}h}{U_s^2}G'(\eta)\eta = f_1' \tag{3.2}$$

primes refer to differentiation with respect to η.

If the flow in the entrainment zone is a self-preserving one, the functions $F(\eta)$, $G(\eta)$ and $f_1(\eta)$ are independent of r, hence the solution of equation (3.2) requires that the coefficient of the universal functions be either zero or non-zero constant [5], [6]. For a non-trivial solution, consider the ratios to be non-zero constant. The non-repetitive coefficients are

$$\frac{dh}{dr}, \frac{h}{U_s}\frac{dU_s}{dr}, \frac{h}{U_s r}\frac{d(U_s r)}{dr}, \frac{g\dfrac{\Delta\rho_s}{\rho_a}h}{U_s^2}\sin\theta, \frac{d\left(g\dfrac{\Delta\rho_s}{\rho_a}\right)}{dr}\frac{h^2}{U_s^2} \tag{3.3}$$

Each of the above coefficients must be equal to a constant, hence

$$h = C_1 r\,, \quad U_s = C_2 r^a\,, \quad \frac{\Delta\rho_s}{\rho_a} = C_3 r^{2a-1} \tag{3.4}$$

and

$$g\frac{\Delta\rho_s}{\rho_a} h/U_s^2 = C_4\,.$$

The above results show that the depth of the layer varies linearly with the radial distance r (i.e. $\sin\theta$ is constant) and the velocity and the density scale varies as a power of r. Equation (3.4) further shows that the sectional Richardon's number, R_i, $(g(\Delta\rho_s/\rho_a)h/U_s^2 = R_i)$, based upon the value of velocity and density scale and the depth of surface layer, remains constant. At this stage no further deduction can be made concerning the exponent a and it is therefore necessary to obtain a further relation if a is to be determined uniquely. These relations can be obtained from equations (2.2) as follows. Equation (2.2) will be integrated with respect to z to give the following equation by making use of the continuity equation and assuming that $\overline{v'\Delta\rho'} = 0$ at $z=0$ and at $z=h$, hence:

$$\frac{d}{dr}\left[\int_0^h \Delta\rho u r\, dz\right] = 0\,. \tag{3.5}$$

By substituting expression (3.1) into equation (3.5) we obtain

$$I_0 \frac{d}{dr}(\Delta\rho_s U_s h r) = 0 \tag{3.6}$$

where

$$I_0 = \int_0^1 F(\eta)\, G(\eta)\, d\eta\,.$$

The above equation can be written in the following form

$$\frac{\Delta\rho_s}{\rho_a} U_s h r = \text{constant}\,. \tag{3.7}$$

By substituting for $\Delta\rho/\rho_a$, U_s and h the expressions given in equation (3.4) into the above equation it can be seen that the obtained equation can only be satisfied if its exponents equal zero, that is

$$2a - 1 + a + 2 = 0 \tag{3.8}$$

hence

$$a = -\tfrac{1}{3}$$

Thus

$$\left.\begin{aligned} U_s &= C_2 r^{-\frac{1}{3}} \\ \Delta\rho_s/\rho_a &= C_3 r^{-\frac{5}{3}}\,. \end{aligned}\right\} \tag{3.9}$$

By this procedure the power a has been determined without making use of the momentum integral equation which, as shown later, can be derived when equation (2.6) is integrated with

respect to z (see equation (4.5) section 4). Equations (3.9) show that in the region of the entrainment zone, where the assumption of a self-preserving flow is acceptable, the velocity and the density scale decrease as the radius r increases in such a way that with the linear increase of the depth the sectional Richardson's number remains constant.

4. Entrainment

In plumes and jets, the turbulent region, which is of finite extent, grows with the distance downstream of the issuing sources and their edge expands to engulf the surrounding fluid. This will be accepted here as the concept of the entrainment process. Hence this entrainment implies a flow of the underlying fluid into the turbulent surface layer and when the underlying fluid is at rest there is a small inflow velocity perpendicular to the main flow [7]. The mean value of inflow velocity can be determined when the continuity equation (2.3) is integrated with respect to z, i.e.

$$\frac{d}{dr}\left[\int_0^h ur\,dz\right] = -v \cdot r \tag{4.1}$$

in which $-v$ is the mean inflow velocity and according to the above concept of the entrainment it is equal to the entrainment velocity, U_e. Hence equation (4.1), by substituting expression (3.1) into it, can be written in the following form

$$I_1 \frac{d}{dr}(U_s h r) = U_e r \tag{4.2}$$

where

$$I_1 = \int_0^1 F(\eta)\,d\eta\,.$$

The above equation shows that the increase of mass of the surface layer in the entrainment zone is due to the entrainment velocity U_e. Substituting for h and U_s from equations (3.4) and (3.9) into equation (4.2) it follows that

$$U_e = C_5 r^{-\frac{1}{3}}\,. \tag{4.3}$$

This shows that the entrainment velocity U_e varies with r in the same way as the velocity scale U_s. Here it will be assumed that the entrainment velocity U_e in the region of self-preserving flow is proportional to the velocity scale U_s. This means that the Reynolds number is high enough for the effect of molecular viscosity to be negligible. Hence we can write

$$\alpha = \frac{U_e}{U_s} = \frac{C_5 r^{-\frac{1}{3}}}{C_2 r^{-\frac{1}{3}}} = \text{constant}\,. \tag{4.4}$$

The above expression shows that the proportionality factor α, or the coefficient of entrainment, in the self-preserving region of the surface layer remains constant. The constant value of the coefficient of entrainment differs for different types of self-preserving flows. For instance in two dimensional and circular momentum jets the value of α is equal to 0.075 and 0.07 [6], [7]. For a two-dimensional and a circular plume α is 0.16 and 0.082 respectively [8]. Here an attempt is made to determine the factors upon which the coefficient of entrainment may depend.

Equation (2.6) can be integrated with respect to z to give the following equation by considering that the integral of the Reynolds shear stress is zero at $z=0$ and at $z=h$. Hence

$$\frac{d}{dr}\left[\int_0^h \rho u^2 r\,dz\right] = -\left[\int_0^h g(\rho_a-\rho) r\,dz\right] \sin\theta + \frac{d}{dr}\left[\int_0^h g(\rho_a-\rho) rz\,dz\right]. \tag{4.5}$$

The left-hand side of the above equation can be derived when the integration is carried by parts and by making use of the continuity equation (2.3).

Multiplying equation (2.6) by velocity U, and integrating with respect to z, also by making

use of the continuity equation when the integration is carried by parts, the following equation is obtained [6].

$$\frac{d}{dr}\left[\int_0^h \tfrac{1}{2}\rho u^3 r\,dz\right] = \left[\int_0^h g(\rho_a-\rho)ur\,dz\right]\sin\theta + \frac{d}{dr}\left[\int_0^h g(\rho_a-\rho)urz\,dz\right]. \tag{4.6}$$

The above equation, in fact, is an expression of mechanical energy in the r-direction and it gives the relation between the rate at which energy of the flowing fluid changes and the rate at which work must be done to cause these changes [9], [10]. Substituting for u and $(\rho_a-\rho)$ the expressions given in equation (3.1) into equations (4.5) and (4.6) it follows that

$$I_2\frac{d}{dr}(U_s^2 hr) = -I_3\left(g\frac{\Delta\rho_s}{\rho_a}hr\right)\sin\theta + I_4\frac{d}{dr}\left(g\frac{\Delta\rho_s}{\rho_a}h^2 r\right) \tag{4.7}$$

$$I_5\frac{d}{dr}(U_s^3 hr) = -2I_0\left(g\frac{\Delta\rho_s}{\rho_a}U_s hr\right)\sin\theta + 2I_6\frac{d}{dr}\left(g\frac{\Delta\rho_s}{\rho_a}U_s h^2 r\right) \tag{4.8}$$

in the above equations

$$\left.\begin{aligned} I_2 &= \int_0^1 F^2(\eta)d\eta\,, \quad I_3 = \int_0^1 G(\eta)d\eta\,, \quad I_4 = \int_0^1 G(\eta)\eta\,d\eta \\ I_5 &= \int_0^1 F^3(\eta)d\eta\,, \quad I_6 = \int_0^1 F(\eta)G(\eta)\eta\,d\eta\,. \end{aligned}\right\} \tag{4.9}$$

Equation (4.8) can be written in the following form

$$2U_s\frac{d(U_s^2 hr)}{dr} - U_s^2\frac{d(U_s hr)}{dr} = -2\frac{I_0}{I_5}\left(g\frac{\Delta\rho_s}{\rho_a}U_s hr\right)\sin\theta + 2\frac{I_6}{I_5}\frac{d}{dr}\left(g\frac{\Delta\rho_s}{\rho_a}U_s h^2 r\right). \tag{4.10}$$

Multiplying equation (4.7) by $2U_s$ and substituting into equation (4.10) the following equation is obtained

$$\frac{d(U_s hr)}{dr} = -A_1 g\frac{\Delta\rho_s}{\rho_a}\frac{hr}{U_s}\sin\theta - A_2\frac{1}{U_s^2}\frac{d}{dr}\left(g\frac{\Delta\rho_s}{\rho_a}U_s h^2 r\right) + A_3\frac{1}{U_s}\frac{d}{dr}\left(g\frac{\Delta\rho_s}{\rho_a}h^2 r\right) \tag{4.11}$$

where

$$A_1 = 2\left(\frac{I_3}{I_2} - \frac{I_0}{I_5}\right), \quad A_2 = 2\frac{I_6}{I_5} \quad \text{and} \quad A_3 = 2\frac{I_4}{I_2}$$

all of which are numerical constants.

On comparing equation (4.11) with equation (4.2) and considering equation (4.4) the following expression, with suitable rearrangement, can be derived for the coefficient of entrainment, i.e.

$$\alpha = \frac{U_e}{U_s} = -I_1 A_1 R_i\sin\theta - I_2 A_2\frac{1}{U_s^3 r}\frac{d}{dr}(U_s^3 hr R_i) + I_1 A_3\frac{1}{U_s^2 r}\frac{d}{dr}(U_s^2 hr R_i) \tag{4.12}$$

where R_i is the Richardson's number and is constant (see Section 3 equation (3.4)). By substituting for U_s and h from equation (3.9) and (3.4) into equation (4.12) and replacing constant C_1 by $\sin\theta$ it gives

$$\alpha = I_1(-A_1 - A_2 + \tfrac{4}{3}A_3)R_i\sin\theta\,. \tag{4.13}$$

Equation (4.13) shows that the coefficient of entrainment depends on the Richardon's number and also the slope of the interface. Hence the value of α remains constant for each experimental run. The above equation shows that the value of α for a given R_i is maximum when $\theta = \pi/2$ and the entrainment is negligible when the interface is horizontal. The numerical values of I_1 and A_1–A_3, which in turn depend upon the definition of functions $F(\eta)$ and $G(\eta)$, can be determined by using equations (7.13) and (7.14), which were determined from velocity and density profiles

obtained from the experimental measurements. However, the numerical values are:

$$I_1 = 0.625\,, \quad A_1 = 0.204, \quad A_2 = 1.676 \quad \text{and} \quad A_3 = 1.646$$

By substituting the above values and also for U_s and h from (3.9) and (3.4) into equation (4.13)

$$\alpha' = 0.197\, R_i \sin\theta \tag{4.14}$$

The value of θ did not exceed 5° and R_i for all experimental runs varies between 0.62 and 0.86, hence the value of α is less than 0.0148. This value of α agrees reasonably well with the experimental results of Ellison et al. [7].

5. Zone of Homogeneous Flow

Beyond some radius r_e (see Fig. 1) the velocity, U_s, becomes small, and entrainment is negligible. This means that the interface becomes horizontal ($\theta \approx 0$ see Section 3). The surface layer beyond the "entrainment zone" moves into a new zone in which the layer travels over the underlying pool, behaving much like homogeneous flow over a level surface. The surface layer in this zone is affected only by gravitational and inertial forces. The density and velocity is first assumed to be uniform throughout the layer with a discontinuity at the interface. This simplified approach helps the interpreting of experimental results, some deviation between the results of the analysis and experiment being anticipated due to those secondary aspects which would have to be considered in a precise quantitative analysis. However, the approach also entails the assumption that the thickness of the surface layer remains constant, the density of the layer equalling that at the end of the entrainment zone (see Fig. 1).

Let U_i be the velocity at radius $r_i = r_e$ and h_i the thickness of the layer. Then the relationship to the buoyancy flux, B, (see also Equation (3.7)) at radius r_e can be written as follows:

$$2\pi r_i h_i U_i g(\rho_a - \rho_i) = B \tag{5.1}$$

where ρ_i is the density of the surface layer in the zone of homogeneous flow. All terms in equation (5.1) are constant except r_i and U_i, hence we can write

$$U_i r_i = \frac{B}{2\pi h_i g(\rho_a - \rho_i)} = C\,. \tag{5.2}$$

The above equation indicates that the velocity decreases inversely with the increase of radius. By substituting $U_i = dr_i/dt$, where t is the displacement time, into equation (5.2) it follows

$$r_i \frac{dr_i}{dt} = C \tag{5.3}$$

subject to the boundary condition

$$r_i = r_e, \quad t = t_e\,. \tag{5.4}$$

By integrating equation (5.3) with the use of (5.4) we obtain the following equation:

$$r_i - r_e = (2C)^{\frac{1}{2}}(t - t_e)^{\frac{1}{2}}\,. \tag{5.5}$$

In order to compare the experimental results with the above equation, the value of C needs to be defined in the case of a real fluid, when a boundary layer exists adjacent to the interface between the two-layered fluid. One effect of the boundary layer is to cause a displacement to the external flow (potential flow), which will probably have to be taken into account when experimental results are compared with the simplified theory. The actual thickness h_i can be expressed as

$$h = h_i + h^* \tag{5.6}$$

where h^* is the displacement thickness by which the potential flow of the thickness, h_i, is forced away from the interface (see Fig. 1). By substituting equation (5.6) into equation (5.2) the following relation can be obtained:

$$\frac{B}{2\pi[g(\rho_a-\rho_i)h-g(\rho_a-\rho_l)h^*]} = C \tag{5.7}$$

where ρ_l is the mean value of density in the layer of thickness, h^*. Experiments possibly show that the second term in the denominator of equation (5.7) is small and can be neglected in comparison with the first term: B can be determined by calculating the velocity U_s (see equation (3.10) and also section 7) at a radius r where α becomes negligible.

6. Experiments

Installation and measurements

A tank $16 \times 16 \times 6$ ft deep was filled with fresh water, to which salt was added to give the required concentration of 25 g/l. A homogeneous solution was obtained by running a 6 cusec pump, which sucked the salt solution from a bottom corner of the tank and fed it back to the tank at two different places on the floor of the tank. The density was measured at various points using a Princeton electrical conductivity probe whilst the pump was running. An experiment was not started until at least 4 hours had elapsed, by which time all disturbance caused by the mixing process had died out. The density and temperature of the solution were checked before each experiment.

The buoyant jet consisted of fresh water discharged from a 1 in. diameter nozzle. This was supplied from a header tank with overflow, thus providing a constant head. The discharge was registered by a variable-orifice flow meter of commercial design. The temperature of the ambient fluid and effluent were matched during each experimental run.

The velocity of the surface layer was measured photographically, viewing with a cine camera above the tank. By placing a temporary square grid at the water surface the scale of the film was obtained. Two methods were used to measure the velocity of the surface layer.

First, methylene blue organic dye (concentration 40 mg/l) at the required temperature was injected into the pipe feeding the effluent nozzle. This method gave the velocity of the tip of the surface layer. The second method was adopted in order to measure the velocity of the surface layer behind the tip. Buoyant white coloured balls of 0.9 in. diameter were placed at the free surface of the layer at short intervals. This method proved very convenient and hence was used throughout the experimental work. The velocity distribution through the depth of the surface layer was obtained by means of a miniature current meter.

The density at points in the surface layer was deduced from the concentration using the Princeton probe in situ. The diameter of this probe was $\frac{3}{16}$ in tapered to $\frac{1}{16}$ in. at the electrode. The probe measured the turbulent fluctuation of conductivity, from which the mean value was determined by inspection.

The slope of the free surface of the surface layer in the zone of homogeneous flow was measured as follows. Silver nitrate was sprayed uniformly on a strip of paper one inch wide, together with a layer of potassium chromate. When such a paper strip is partly immersed in salt solution, it turns white (silver chlorate) with a sharp line indicating the free surface. The prepared strips were first placed one foot apart dipping into the ambient salt solution from a firm bridge. The sharp line indicating the horizontal free surface before the experimental run was marked with a fine pencil line. After an experiment, the division between the bright and dark colouration indicated the free surface of the spreading layer. The surface layer slope could then be determined from the marks on the paper strips.

7. Experimental Results

It was shown in Section 3 that the velocity and the density scales vary as powers of radius distance r from the virtual origin and are of the form given in equation (3.9). This equation may be written as

$$U_s = C_2(r_0+r')^{-\frac{1}{3}} \tag{7.1}$$

and

$$\Delta\rho_s/\rho_a = C_3(r_0+r')^{-\frac{5}{3}} \tag{7.2}$$

where r_0 is the radius distance from the beginning of the surface layer (point O in Fig. 1) to the point where the turbulence is assumed to originate (virtual origin). The values of the constants C_2 and C_3 and also of the virtual origin r_0 need to be determined.

Since the velocity and the density scales are functions of radius r, and variables U_0, h_0 (the velocity and the depth of the surface layer at section O) $\Delta\rho_b$ (the density differences at the boil, $\Delta\rho_b=\rho_b-\rho_a$) and g. Here it will be assumed, as was also confirmed experimentally, that the density in the hatched area in Fig. 1 is equal at the boil. Dimensional analysis shows that the dependent variables U_s, $\Delta\rho_s$ and h can be expressed in the following forms

$$\frac{U_s}{U_0} = f_1\left(\frac{r}{h_0}, F_0\right) \tag{7.3}$$

$$\frac{\Delta\rho_s}{\Delta\rho_b} = f_2\left(\frac{r}{h_0}, F_0\right) \tag{7.4}$$

$$\frac{h}{h_0} = f_3\left(\frac{r}{h_0}, F_0\right) \tag{7.5}$$

where

$$F_0 = U_0/(gh_0\Delta\rho_b/\rho_a)^{\frac{1}{2}}\,.$$

Equation (7.3) can be written in the following form by using equation (3.9)

$$\frac{U_s}{U_0} = (r/h_0)^{-\frac{1}{3}}\varphi_1(F_0)\,. \tag{7.6}$$

Similarly equation (7.4) gives

$$\frac{\Delta\rho_s}{\Delta\rho_b} = (r/h_0)^{-\frac{5}{3}}\varphi_2(F_0)\,. \tag{7.7}$$

On comparing equations (7.6) and (7.7) with equation (3.9) it is found that

$$C_2 = U_0 h_0^{\frac{1}{3}}\varphi_1(F_0) \tag{7.8}$$

and

$$C_3 = \frac{\Delta\rho_b}{\rho_a} h_0^{\frac{5}{3}}\varphi_2(F_0)\,. \tag{7.9}$$

The velocity and density scale were assumed to be the maximum values of these quantities which occur near the surface for each section. The measured values of velocity were compared with equation (7.6) by considering equation (7.8) it was found that the equation (7.6) can be written in the following form

$$\frac{U_s}{U_0} = 1.19\left(\frac{r'}{h_0} + 1.7\right)^{-\frac{1}{3}} \tag{7.10}$$

in which it was assumed, and also confirmed experimentally, that the initial depth $h_0 \approx r_p$, where r_p is the plume radius at height H (see Fig. 1) and $U_0 = Q_0 S_0/2\pi h_0^2$ where $S_0 = \rho_a - \rho_0/\rho_a - \rho_b$ and Q_0 is the flux from the nozzle having density ρ_0. Equation (7.10) together with the experimental measurements for various initial densimetric Froude numbers F_0 are shown in Fig. 2. Similarly it was found that equation (7.7) can be written in the following form

$$\frac{\Delta\rho_b}{\Delta\rho_s} = 0.245\left(\frac{r'_1}{h_0} + 2.3\right)^{\frac{5}{3}} \tag{7.11}$$

It should be noted that equation (7.11) is the reciprocal of equation (7.7) and is written in this

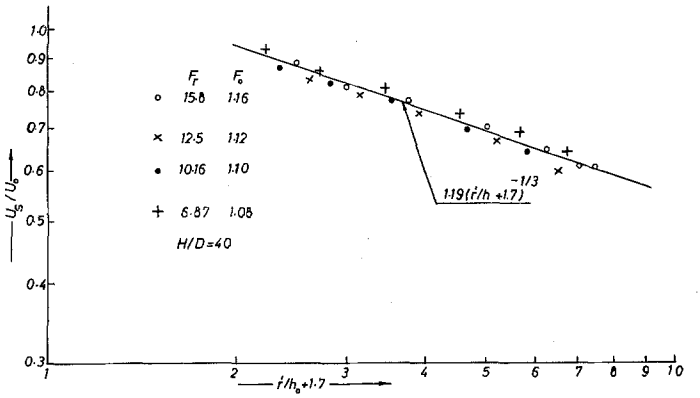

Figure 2. Distribution of velocity scale in the entrainment zone.

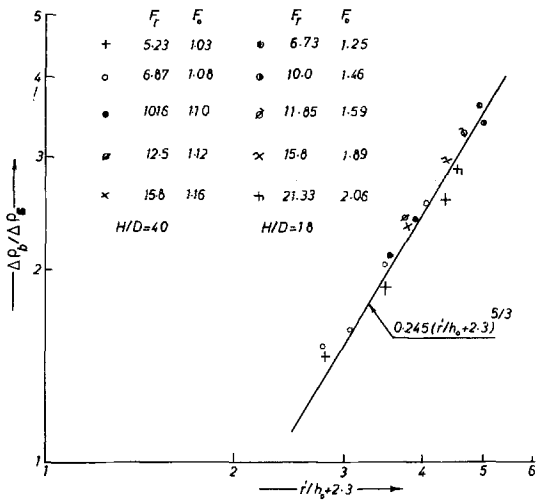

Figure 3. Dilution of the surface layer in the entrainment zone.

form because of its practical use. However, equation (7.11), together with the experimental results, are shown in Fig. 3. On comparing (7.11) with (7.10) it can be seen that the radius of the virtual origin for the non-dimensional velocity U_s/U_0 differs from that of the non-dimensional density $\Delta\rho_b/\Delta\rho_s$. This means that the dilution of the surface layer will start when $U/U_0 = 1.11$ or $r'_1/h_0 = r'/h_0 + 0.5$.

7.1 *Velocity*

The times taken for the white buoyant balls to travel to various radii were measured from the film, and evaluated according to equation (5.5). If the assumption used for deriving equation (5.5) is correct where $r_i > r_e$, and the flow condition is that of an inviscid fluid, then the points should fall on a straight line when the values of r_i are plotted against $(2C)^{\frac{1}{2}}t^{\frac{1}{2}}$, the inclination of the line being 45°. This plot can be seen in Figs. 4 and 5 for non-dimensional submergence height of $H/D = 18$ and 40. It appears that the zone of homogeneous flow of constant depth occurs in the region when $r_i > 30$ approximately for the case considered here. When $r_i < 30$ the plotted data deviate from the 45° straight line indicating that radial velocity is not inversely proportional to radius. The variation of $2C$ with F_r for the cases given in Figs. 4 and 5 are shown in Fig. 6. F_r is the nozzle densimetric Froude number defined as

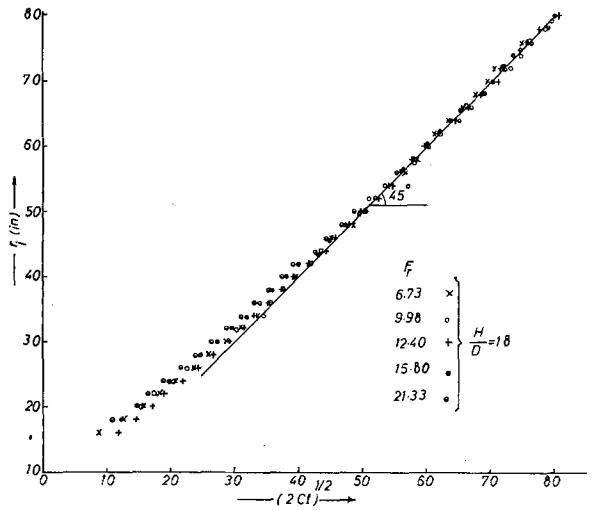

Figure 4. Length time curve of the surface layer in the zone of homogeneous flow for $H/D=18$.

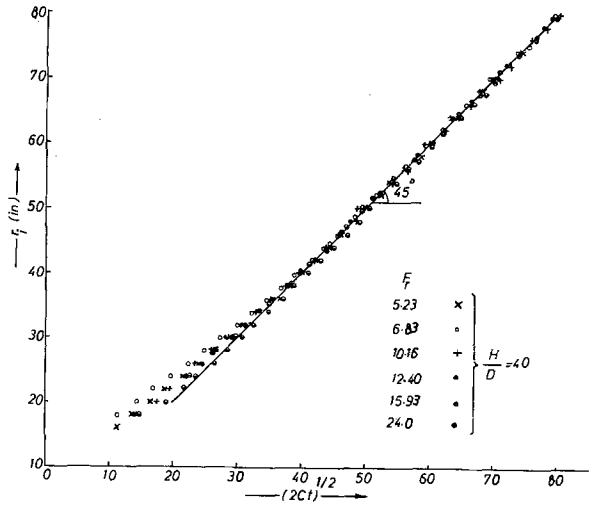

Figure 5. Length time curve of the surface layer in the zone of homogeneous flow for $H/D=40$.

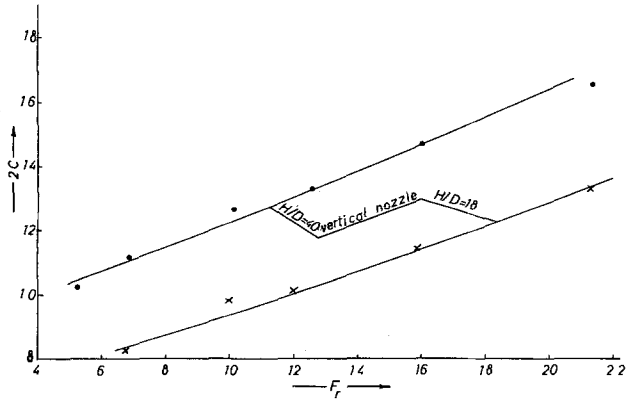

Figure 6. Variation of constant C of Eq. (5.2) with nozzle densimetric Froude number F_r.

$$F_r = \frac{Q_0}{\pi \frac{D^2}{4}\left(g\frac{\rho_a - \rho_0}{\rho_a} D\right)^{\frac{1}{2}}} \tag{7.12}$$

where D is the nozzle diameter.

In one experiment the dye technique was combined with the use of buoyant balls. The results of this experiment are shown in Fig. 7, which shows the velocity of the tip and the zone behind the tip. On comparing the two curves in this figure it can be seen that the balls travel faster than the tip of the dye ($C_{\text{ball}} > C_{\text{dye}}$). The fact that the radial velocity is inversely proportional to radius beyond $r_i = 30$ in. is also confirmed.

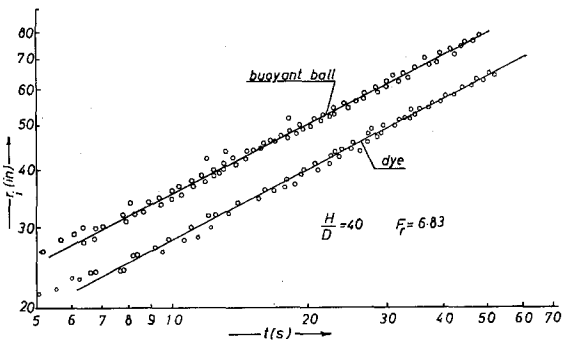

Figure 7. Length time curve for the tip and behind the tip.

It was also observed that the dye front in the zone of homogeneous flow tended to diffuse sideways and it is believed that this may have been due to incomplete homogeneity of the ambient fluid. The motion of the balls following a short distance behind the tip was always in a radial direction.

7.2. *Density Profile*

Fig. 8 shows the density profile plotted non-dimensionally in the entrainment zone at various radii for two nozzle densimetric Froude numbers, $F_r = 5.23$ and 6.87. In it is also shown a fitted expression for functions $G(\eta)$ i.e.

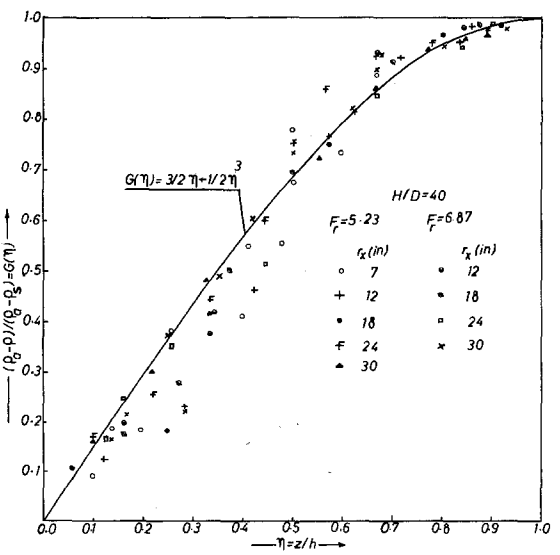

Figure 8. Density distribution in the entrainment zone.

$$G(\eta) = \tfrac{3}{2}\eta - \tfrac{1}{2}\eta^3 \,. \tag{7.13}$$

The above function and the one for the velocity profile (defined later) was used to determine the value of the integrals given in equation (4.9). Although other expressions could be found with a better fit to the experimental data, they would not cause any significant change to the value of integrals, which was used to evaluate the constants in equation (4.13).

Fig. 9 shows the non-dimensional density profile measured in the zone of homogeneous flow for various values of F_r and a difference will be noted from those given in Fig. 8, because they relate to a different type of flow. Fig. 9 shows less variation of density in the moving part of the depth of the layer than in the entrainment zone.

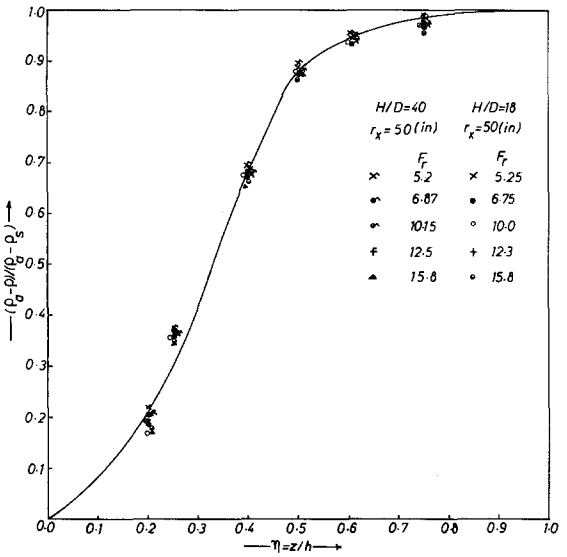

Figure 9. Density distribution in the zone of homogeneous flow.

The distinction between the zones is even more apparent in Fig. 10. Fig. 10a shows the typical pictures of density fluctuation at points in the turbulent zone using the conductivity probe described before, and Fig. 10b shows the results obtained in the zone of homogeneous flow, where density fluctuations were not observed even when the recording time was increased from 20 seconds to 45 seconds.

7.3. *Velocity Profile*

The results of measurements with a miniature current meter for nozzle densimetric Froude numbers $F_r = 5.23$ and $F_r = 6.87$ are shown non-dimensionally in Fig. 11. It was rather difficult to obtain more experimental data with the current meter when the velocity was low. It was also impossible to obtain satisfactory velocity measurements for high values of F_r because the time to run such an experiment was too short. However, the following expression

$$F(\eta) = \tfrac{3}{2}\eta - \tfrac{1}{2}\eta^3 \tag{7.14}$$

is given in this figure, which shows a fair agreement with the experimental data. Equations (7.13) and (7.14) show that the functions are zero and 1 when $\eta = 0$ and $\eta = 1$ respectively, and furthermore have a horizontal tangent at $\eta = 1$.

7.4. *Final Thickness of the Surface Layer*

Experiments with a vertical nozzle showed that the final thickness of the moving layer ($h =$

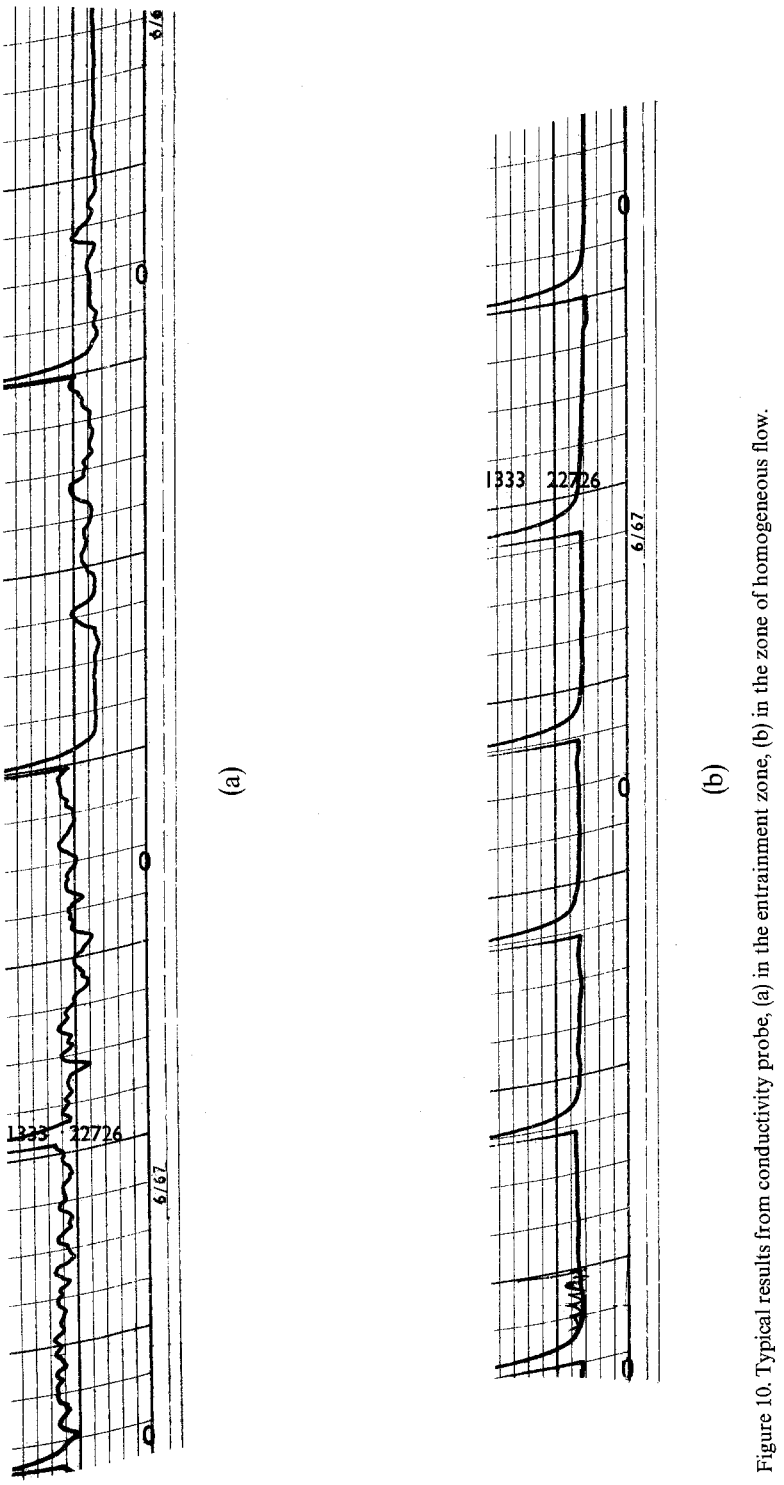

Figure 10. Typical results from conductivity probe, (a) in the entrainment zone, (b) in the zone of homogeneous flow.

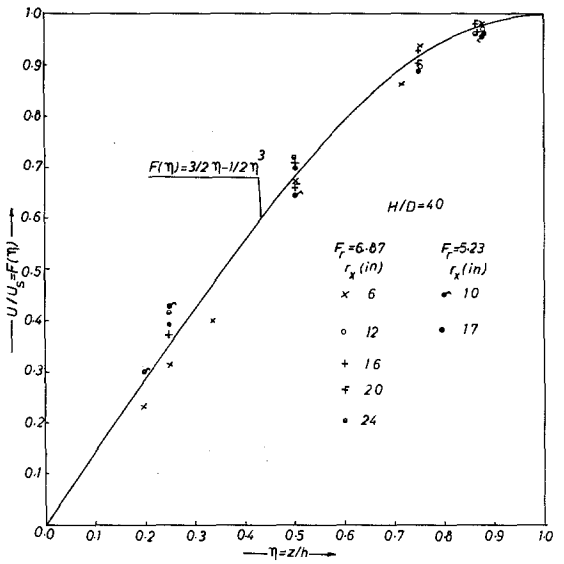

Figure 11. Velocity distribution in the entrainment zone.

h_i+h^*, see equation (5.6)) depends on the submergence height H. Measured values of h, for all values of the densimetric Froude number F_r shown in Fig. 9 was 1.38 in. when H was 18 in. and hence $h/H \approx \frac{1}{13}$ in this case. When the submergence height H was increased to 40 in. the final thickness h for all values of F_r given in Fig. 9 increased to 2.37 in., which gives $h/H \approx \frac{1}{17}$. Thus, although the final thickness of the surface layer increases with the increasing H, h/H does not remain constant. In other words, when the submergence height H increases by, say, 100% the value of h increases by 70% only. This, of course, cannot be applicable for all cases and probably the ratio h/H approaches a constant value for values of $H > 40$ in. The higher value of h/H (i.e. $h/H > \frac{1}{13}$) may be a simple scale effect, or h/H may depend on H/D. However, the above results should be accepted with reserve and more experimental work is necessary to establish its validity.

7.5. *Surface Slope*

Slopes, S, of the surface layer were measured for various F_r values when the tip of the moving layer was about 5 in. from the wall of the tank. The measurements showed that in the zone of homogeneous flow $S \approx 0.00165$ when the submergence was 18 in. and $S \approx 0.00195$ when $H =$ 40 in. The measurements did not indicate any surface slope in the entrainment zone.

Acknowledgement

The work described herein was carried out as part of a research programme of the Hydraulics Research Station, and the paper is published by permission of the Director of Hydraulics Research. The writer wishes to express his thanks to J. A. Weller for his help in measurement.

REFERENCES

[1] A. M. Rawn and H. K. Palmer, Pre-determining the extent of a sewage fluid in sea water, *Transactions, A.S.C.E.*, 94 (1930) 1036–1060.
[2] W. E. Hart, Jet discharge into a fluid with a density gradient, *Proc. A.S.C.E.*, 87, No. HY6, (1961) 171–200.
[3] J. J. Sharp, Spread of buoyant jet at the free surface, *Proc. A.S.C.E.*, 95, No. HY3, (1969) 811–835.
[4] G. K. Batchelor, The conditions for dynamical similarity of motion of a frictionless perfect-gas atmosphere, *Quart. J. Royal Met. Soc.*, 79 (1953) 224–235.
[5] J. O. Hinze, *Turbulence*, McGraw-Hill Book Comp. Inc. (1959).

[6] A. A. Townsend, *The structure of turbulent shear flow*, Cambridge University Press (1956).
[7] T. H. Ellison and J. S. Turner, Turbulent entrainment in stratified flows, *J. Fluid Mech.*, 6 (1959) 423–448.
[8] H. Rouse, C. S. Yih and H. W. Humphreys, Gravitational convection from a boundary source, *Tellus* 4 (1952) 201–210.
[9] H. Rouse, ed., *Advanced Mech. of Fluids*, London, Chapman and Hall, (1959).
[10] D. G. Fox, *Turbulent gravitational convection in a stratified fluid*, Ph.D. Thesis Princeton University, (University Microfilms, Ann Arbor) (1968).